

C. Herta · H. Winkler · R. Benda · M. Haas
A.X. Trautwein

Dynamic structural disorder of the FeO₂ moiety in oxymyoglobin studied by nuclear resonant forward scattering of synchrotron radiation

Received: 10 January 2002 / Revised: 6 May 2002 / Accepted: 16 May 2002 / Published online: 12 July 2002
© EBSA 2002

Abstract Oxy- as well as deoxymyoglobin exhibit a pronounced temperature dependence of the quadrupole splitting of the heme iron as detected by conventional Mössbauer spectroscopy. With nuclear resonant forward scattering (NFS) of synchrotron radiation, which can be viewed as Mössbauer spectroscopy in the time domain, it is shown that this spectroscopic behavior, although it is phenomenologically similar in the two cases, is based on completely different physical mechanisms. It is demonstrated that stochastic fluctuations of the iron electric field gradient in MbO₂, which are due to the dynamic structural disorder of the FeO₂ moiety, are the reason for the temperature-dependent alterations of the coherent quantum beat pattern in the NFS spectra of MbO₂, in contrast to deoxyMb where transitions between orbital states of iron take place. This subtle spectroscopic difference cannot be inferred from conventional Mössbauer spectroscopy.

Keywords Nuclear resonant forward scattering · Oxymyoglobin · Dynamic structural disorder

Abbreviations *EFG*: electric field gradient · *Mb*: myoglobin · *MSD*: mean square displacement · *NFS*: nuclear resonant forward scattering

Introduction

Myoglobin (Mb) has intensively been studied because of its important physiological role as an oxygen storage protein. Mb is an iron heme protein with one heme

group per molecule. An oxygen molecule can be bound reversibly to the heme iron. Conventional Mössbauer spectroscopy has provided information about the electronic structure of this bond (Bade and Parak 1978; Spartalian and Lang 1980; Maeda et al. 1981).

Oxymyoglobin (MbO₂) as well as deoxymyoglobin (deoxyMb) exhibit a pronounced decrease of the quadrupole splitting ΔE_Q with increasing temperature, as detected by conventional Mössbauer spectroscopy (Boso et al. 1984). In deoxyMb the pentacoordinate heme iron is in the spin quintet ($S=2$) electronic configuration, which allows transitions between various electronic configurations within the t_{2g} subspace with increasing temperature, thus giving rise to a decrease of ΔE_Q (Eicher et al. 1976). For MbO₂, in contrast, it is known that the net spin of the iron oxygen moiety is zero, but it is not so certain whether the iron and the dioxygen themselves are diamagnetic with $S=0$ or whether the iron is in the ferric low-spin state with $S=1/2$ coupled antiparallel with the spin doublet of peroxide, O₂[−]. The latter case of a formal Fe^{III}-O₂[−] bond would give the possibility to explain the rather large quadrupole splitting of 2.3 mm s^{−1} at 4.2 K and also its strong temperature dependence, as has been done by Bade and Parak (1978) in the framework of ligand field theory. MO calculations by Herman and Loew (1980) have confirmed this model in so far as one of the d electrons of iron is found to be asymmetrically delocalized so much that a Fe^{III}(d⁵)-O₂[−] description seems to be appropriate. However, as far as the spin state of the FeO₂ moiety is concerned, it is a true diamagnetic singlet while the first excited “antiferromagnetic” singlet is 13,500 cm^{−1} above this diamagnetic ground state. The asymmetric delocalization can describe the large absolute value of the quadrupole splitting as well as its variation with temperature, but not the asymmetric broadening of both lines of the quadrupole doublet which is observed with increasing temperature. There exists strong evidence that some dynamic structural disorder of the FeO₂ moiety is the reason for the temperature dependence of the quadrupole splitting, as suggested for FeO₂

C. Herta · H. Winkler (✉) · R. Benda · A.X. Trautwein
Institut für Physik, Medizinische Universität zu Lübeck,
Ratzeburger Allee 160, 23538 Lübeck, Germany
E-mail: winkler@physik.mu-luebeck.de
Fax: +49-451-5004214

M. Haas
Institute of Physics, University of Tartu, Riia 142,
2400 Tartu, Estonia

“picked-fence” porphyrins by X-ray and conventional Mössbauer studies (Spartalian et al. 1975; Schappacher et al. 1987). Even though steric hindrance prevents this type of disorder in MbO_2 , a restricted structural disorder of the terminal O-atom was proposed also for MbO_2 by Phillips (1980). However, other than with the picket-fence model, the interpretation of Mössbauer spectra taken of the native protein has not yet been carried out. In the present work we present temperature-dependent studies of oxygenated Mb by means of nuclear resonant forward scattering (NFS) of synchrotron radiation.

In NFS the decay of collectively excited states of the iron nuclei, i.e. of the so called “nuclear exciton” (van Bürc et al. 1992; Kagan 1999), is observed. Stochastic fluctuations of hyperfine parameters, e.g. of the electric field gradient (EFG), destroy the coherence within the nuclear exciton and thus give rise to a faster decay of the intensity of the time-delayed NFS with increasing temperature (Smirnov and Kohn 1995). This drop in intensity is a more reliable indicator for the presence of dynamic molecular properties than any changes of the lineshapes in conventional Mössbauer absorption spectra, because the lineshape can be influenced easily by insufficiencies of the experimental setup. It is therefore expected that one can distinguish between the two cases mentioned above, the static EFG in deoxyMb and the dynamic EFG in MbO_2 , by NFS.

Materials and methods

The samples of Mb were prepared as described by Keppler et al. (2000). The deoxyMb had a pH of 6.5 and the MbO_2 a pH of 7.8. The experiments were performed at the beamline BW4 of the Hamburg synchrotron laboratory (HASYLAB). The measurements were carried out in the “2-” and “5-bunch” mode. The time spacing between two bunches is about 500 ns in “2-bunch” and 200 ns in “5-bunch” mode. The radiation, which has the same time structure as the positron bunches in the storage ring, was monochromatized to a very small bandwidth of the order of some meV at the Mössbauer energy E_γ of 14.4 keV. This had been done in order to avoid overloading of the detector and to reduce radiation damage in the protein. The X-ray pulses were transmitted through the sample, which had a size of 12 mm×2 mm (width×height) and was placed in a liquid helium cryostat. The time-delayed signal from the sample was then detected by fast APD detectors (Baron 1995), analyzed by fast electronics and recorded with a computer.

The simulations of the spectra were performed with the program package SYNFOSS (Haas et al. 1997, 2000a), which allows the simulation of NFS spectra including powder averaging as well as paramagnetic relaxation and fluctuation of the EFG (Leupold and Winkler 1999; Haas et al. 2000b). For the fitting of the experimental spectra with SYNFOSS, an appropriate routine was developed. The goodness-of-fit was judged by the non-weighted equation:

$$\chi^2 = \sum_{i=1}^N (Y_i - g(\mathbf{a}, t_i))^2 \quad (1)$$

with Y_i being the measured count rate in channel i corresponding to the delay time t_i , and $g(\mathbf{a}, t_i)$ being the value of the simulated spectrum with parameter vector \mathbf{a} at time t_i ; for instance: $\mathbf{a} = (\Delta E_Q, t_{\text{eff}})$.

The experimental background (noise) was determined as 0.03 Hz. By scanning the sample with a narrow synchrotron beam

(about 1 mm×0.3 mm) the homogeneity of the effective thickness was determined as $\pm 2.5\%$. Though the homogeneity of the sample was shown to be relatively high, care was taken that at each temperature the synchrotron beam was hitting the sample at the same position. In the case of stochastic fluctuations, the parameters “effective thickness” and “relaxation rate” are strongly correlated in the fit. Therefore a model for the temperature dependence of the effective thickness has been used. In this model the effective thickness t_{eff} is the product of a temperature-independent factor C and the Lamb-Mössbauer factor $f(T)$:

$$t_{\text{eff}} = C \cdot f(T) \quad (2)$$

The temperature-dependent f -factor is generally given by

$$f(T) = \exp(-k\langle x^2 \rangle) \quad (3)$$

with k representing the wave number of the radiation and $\langle x^2 \rangle$ the mean-square displacement (MSD) of iron. In the Debye model, $f(T)$ is approximated by:

$$f(T) = \exp \left\{ -\frac{6E_R}{k_B \Theta_D} \left[\frac{1}{4} + \left(\frac{T}{\Theta_D} \right)^2 \int_0^{\frac{\Theta_D}{T}} \frac{x}{e^x - 1} dx \right] \right\} \quad (4)$$

with $E_R = E_\gamma^2/2mc^2$ being the recoil energy if m is the mass of the iron atom. In this approach, only the parameter Θ_D is needed to describe the variation of the effective thickness with temperature. C is yielded by a low-temperature spectrum, e.g. at $T=3.2$ K.

Results and discussion

Deoxymyoglobin

Figure 1 shows NFS spectra of our deoxyMb sample in the temperature range 3.2–230 K. The simple quantum beat pattern of the measured intensity over the delay time reflects the fact that the Fe nucleus is subjected only to a quadrupole interaction which amounts to $\Delta E_Q = 2.17 \text{ mm s}^{-1}$. With increasing temperature the frequency of the quantum beats decreases, which reflects the decrease of the quadrupole splitting of the heme iron. The envelope of the spectra is mainly determined by the effective thickness of the sample. For small effective thicknesses the envelope can be approximated by an exponential decay of the measured intensity with time (Haas et al. 1997). Therefore on the semi-logarithmic scale shown in Fig. 1 the slope of the envelope provides the effective thickness (see dashed line for $T=3.2$ K). The slower decay with increasing temperature corresponds to a decrease of the effective thickness or, which is equivalent, to an increase of the MSD with temperature. The Debye model according to Eq. (4) was used to describe this behavior. All measured spectra were fitted simultaneously to derive the parameters Θ_D and ΔE_Q . In contrast to ΔE_Q , which is allowed to vary with temperature, C and Θ_D are kept constant over the whole temperature range. An initial value for C was obtained by a fit of the low-temperature spectrum taken at $T=3.2$ K with Θ_D fixed to 200 K, as suggested by conventional Mössbauer measurements. In the final fit, C had to be changed slightly because of a small readjustment of Θ_D that turned out to be necessary in the fits. The spectrum

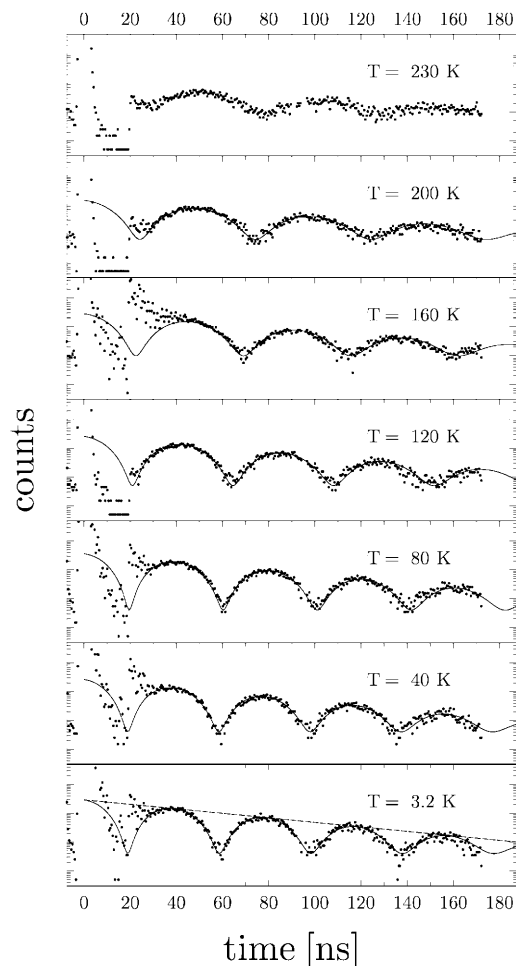


Fig. 1. Measured NFS spectra of deoxyMb at temperatures as indicated. The *solid lines* are the simulations obtained with SYNFOSS using the Debye model for the effective thickness as described in the text

at 230 K was discarded in the fit procedure because above 200 K the effective thickness decreases drastically owing to a significant softening of protein-specific modes (Keppler et al. 2000).

From the simultaneous fit of the spectra in the temperature range 3.2–200 K the Debye temperature was determined as $\theta_D = 215$ K, while ΔE_Q proved to be a temperature-dependent quantity as shown in Fig. 2. This behavior of ΔE_Q obtained here from NFS measurements is in agreement with the results from conventional Mössbauer spectroscopy (Kalvius and Parak 1977), except for the fact that the NFS values for ΔE_Q are systematically 0.1 mm s^{-1} smaller. Since the calibration of our time spectra rests on the bunch-clock signal of the storage ring, we believe that the error margin of our values is less than 1%. The small discrepancy of the absolute values, however, does not invalidate the conclusion of Kalvius and Parak (1977) that a temperature-dependent Boltzmann population of excited orbital states of the heme iron is responsible for the temperature variation of the quadrupole splitting.

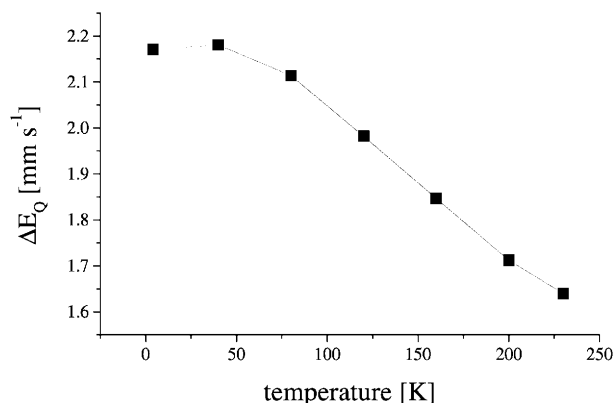


Fig. 2. The temperature dependence of the quadrupole splitting of deoxyMb as obtained from the NFS measurements

MbO₂

The conventional Mössbauer spectrum of our MbO₂ sample taken at 4.2 K is shown in Fig. 3. Besides the fingerprint spectrum of MbO₂, additional subspectra from impurities are visible: 20% metMb and 5% deoxyMb. These additional components must also be allowed for in the NFS simulations of the measured NFS spectra of the MbO₂ sample in the temperature range 3.2–200 K. The parameters for deoxyMb were taken from the analysis discussed above. In order to take the metMb contribution into account, the effect of paramagnetic relaxation (Winkler et al. 1979) was implemented into SYNFOSS (Leupold and Winkler 1999; Haas et al. 2000b). For this purpose the relaxation model of Bizzarri et al. (1995) for the transition probabilities was used and the corresponding parameters for metMb were taken from their work.

In a first step we have analyzed the NFS spectra of our MbO₂ sample in the temperature range 3.2–200 K by allowing only the ΔE_Q of MbO₂ to be fitted. In this

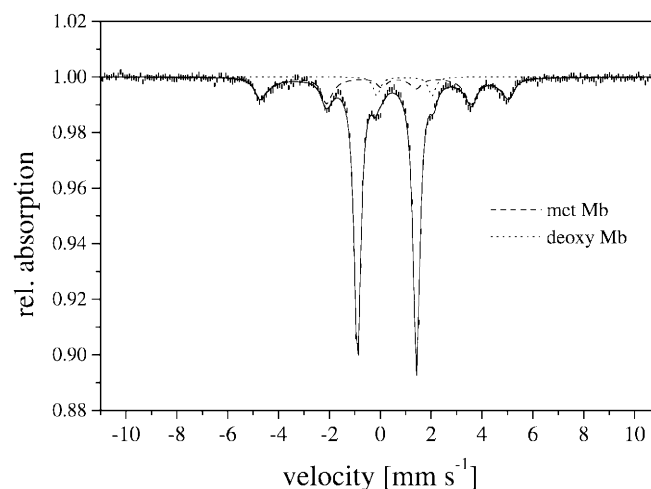


Fig. 3. Conventional Mössbauer spectrum of the MbO₂ sample at 4.2 K

first attempt we have calculated the time-delayed quantum-beat structure of the weighted MbO₂ (75%), met-Mb (20%) and deoxyMb (5%) contributions, assuming the Debye model for the effective thickness of all three components. A reasonable fit was obtained either at the high-temperature end (at 200 K) or at the low-temperature beginning (at 3.2 K) of our series; however, all spectra in the full temperature range could not be fitted simultaneously (results not shown). Therefore in a second approach the effective thickness t_{eff} besides ΔE_Q was also treated as a free parameter. With this procedure a reasonable fit of all spectra in the range 3.2–200 K was obtained; the goodness-of-fit χ^2 (Eq. 1) goes down to 84,822 in this case, which has to be compared with $\chi^2 > 120,000$ obtained in the first step of our analysis. The surprising result of this second approach is that t_{eff} increases with temperature (Fig. 4), which obviously cannot be correct, because the f -factor grows only if $\langle x^2 \rangle$ decreases (see Eq. 3), which should not be the case with increasing temperature.

The obtained result forced us to look for a physically more plausible mechanism in MbO₂ that would influence the NFS spectra in the same way as an increase of the effective thickness does. Large effective thickness causes a fast decay of NFS intensity with delay time. Relaxation has a similar effect on NFS spectra, because dynamic processes cause a dephasing of originally coherent electromagnetic waves and therefore these waves are extinguished at longer delay times (Smirnov and Kohn 1995). The artificial increase of the effective thickness with increasing temperature in MbO₂ (Fig. 4) therefore provides strong evidence that relaxation plays a role. Studies of the FeO₂ moiety in picket-fence porphyrins suggest that relaxation due to dynamic structural disorder of O₂ takes place. This structural disorder was also detected by X-ray diffraction, which shows two or three positions of the terminal O-atom, depending on the kind of picket-fence used (Schappacher et al. 1987). Different positions of the terminal O-atom with respect to the heme iron cause different EFG tensors. The

obtained temperature-dependent quadrupole splitting derived from conventional Mössbauer spectra of FeO₂ in picket-fence porphyrins is a result of stochastic fluctuations of the EFG. It is most likely that the situation in MbO₂ is completely equivalent; this would explain not only (1) the decrease of the ΔE_Q in MbO₂ but also (2) the fast decay of NFS intensity over the delay time with increasing temperature.

The X-ray structure of MbO₂ also exhibits a structural disorder of FeO₂, with two different positions of the terminal O-atom (Phillips 1980). The projection of the O-O bond on the heme plane is rotated by about 40° in position 2 compared to 1. Conventional Mössbauer studies on single crystals of MbO₂ have shown that the principal component V_{zz} of the EFG tensor lies in the heme plane and is oriented along the projection of the O-O bond onto this plane (Maeda et al. 1981). If the terminal O-atom is located in position 2, the EFG should be of the same magnitude as in position 1, but the EFG tensor is rotated accordingly. Therefore the physical picture which we have to envisage is that the EFG fluctuates between two orientations with a rate that depends on temperature. Assuming that the asymmetry parameter η of the EFG in both positions is zero, as in the case of the model compounds, only the rotation angle β between the two EFG tensors must be considered as structural parameter. Considering that $\eta \neq 0$ for the individual EFGs has only a little influence on the analysis, the ratio of the occupation probabilities $p_{1,2}$ of the two positions of the terminal O-atom is given by the Boltzmann factor, with ΔE being the energy difference between these positions:

$$\frac{p_2}{p_1} = \exp\left(-\frac{\Delta E}{k_B T}\right) \quad (5)$$

In the final approach we have fitted the NFS spectra of the MbO₂ sample in the temperature range 3.2–200 K simultaneously by:

1. Treating metMb and deoxyMb as described above.
2. Using the Debye model also for the temperature dependence of the effective thickness t_{eff} of our MbO₂ sample.
3. Letting the EFG tensor fluctuate in MbO₂ between two positions.

This analysis implies the presence of two temperature-independent parameters, i.e. the rotation angle β and the energy difference ΔE , and one temperature-dependent parameter, i.e. the rate w_{12} , by which transitions between positions 1 and 2 occur in the average. The inverse transition rate w_{21} follows from the principle of detailed balance (Winkler et al. 1979):

$$p_1 \cdot w_{12} = p_2 \cdot w_{21} \quad (6)$$

The Debye temperature θ_D was held fixed at 215 K. The result of the global fit of all NFS spectra of MbO₂ is

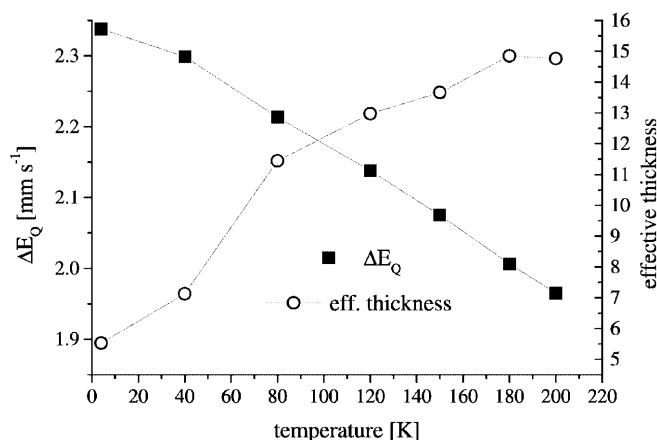


Fig. 4. Effective thickness and ΔE_Q as obtained from the fit of the MbO₂ spectra without consideration of relaxation

shown in Fig. 5. Varying θ_D in the interval 200–250 K does not change the goodness-of-fit χ^2 significantly. From Table 1 it is obvious that the obtained fit parameters β , ΔE and the EFG transition rate are not very sensitive to θ_D .

The variation of the goodness-of-fit χ^2 was analyzed by varying β in the range 30–55° while keeping θ_D at 215 K. With increasing angle β the energy difference ΔE between the two EFG orientations 1 and 2 increases from the value 0 (for $\beta=30^\circ$) to about 188 cm^{-1} (for

$\beta=55^\circ$). The parameter χ^2 reaches a minimum at $\beta \approx 40^\circ$ (Fig. 6). It is worth noting that this value agrees with the result of the X-ray structure determination for MbO_2 (Phillips 1980), where the angle between the two alternative projections of the O-O bond on the heme plane is also found to be about 40° .

The temperature dependence of the EFG transition rates can be interpreted in terms of a low-temperature tunneling plus an activation process to be described by the expression:

$$w_{12}(T) = w_0 \exp\left(-\frac{E_A}{k_B T}\right) + w_T \quad (7)$$

The fit of the data (Fig. 7) yielded $w_0 = 10^9 \text{ s}^{-1}$, $w_T = 10^7 \text{ s}^{-1}$ and an activation energy E_A of $260 \pm 35 \text{ cm}^{-1}$.

One may suppose that our findings are in disagreement with the most recent X-ray structure of MbO_2 published by Vojtěchovský et al. (1999), which exhibits only one position for the terminal oxygen atom at a temperature of 100 K. Actually, the second position should be populated at 100 K by about 17%, if the energy difference between the two positions is chosen as 111 cm^{-1} according to the fit of our NFS measurements. This apparent disagreement can be explained by the high oxygen pressure (100 bar) which had been applied to the myoglobin crystals in that work before the structure of MbO_2 was determined by X-ray diffraction. It is possible that owing to the high oxygen pressure the crystal water molecules are expelled out of the heme pocket. This is indicated by the fact that additional peaks are found in the electron density map, which are assigned to molecular oxygen. Phillips (1980) proposed that exactly the presence of crystal water is responsible for partial occupation of the second position by the terminal oxygen atom, as the water molecules displace the terminal oxygen atom out of its preferred position into the alternate position even though it is higher in energy.

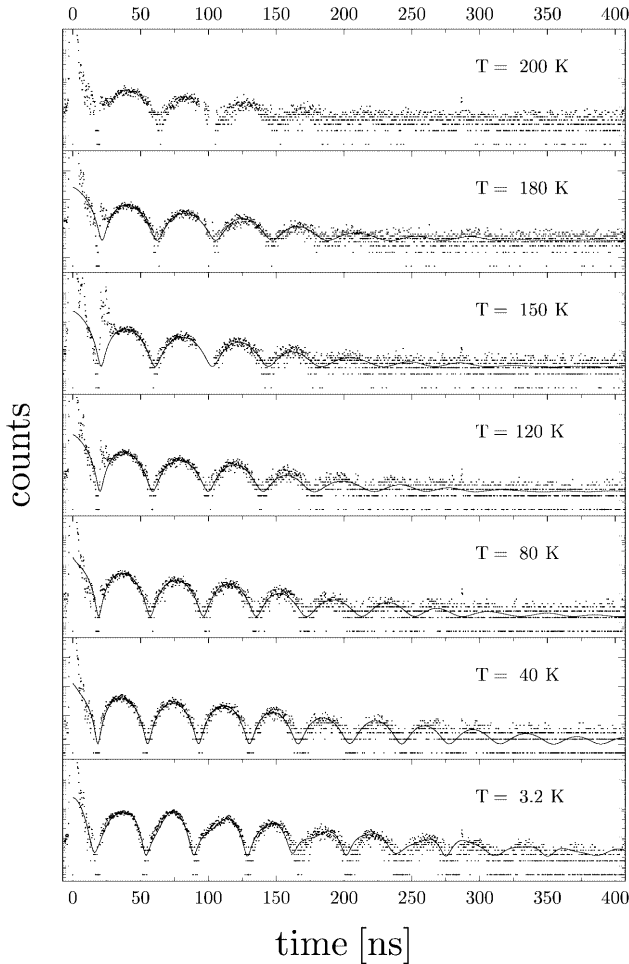


Fig. 5. Measured NFS spectra of the MbO_2 sample. The solid lines result from a simultaneous fit of all experimental spectra, including fluctuations of the EFG tensor. The temperature dependence of the effective thickness is approximated by the Debye model with $\theta_D = 215 \text{ K}$.

Table 1. Goodness-of-fit χ^2 , angle β and energy difference ΔE obtained from the fit at the corresponding Debye temperature θ_D

	θ_D (K)		
	200	215	250
χ^2	87,704	87,670	87,640
β (°)	40.5	40.4	40.5
ΔE (cm^{-1})	111	111	113

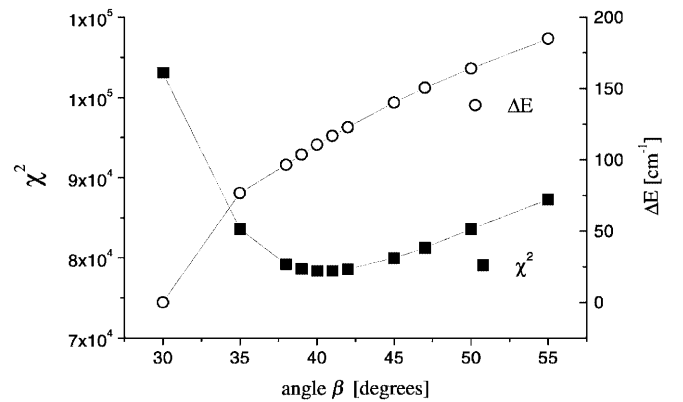


Fig. 6. Dependence of the goodness-of-fit χ^2 and of the energy difference ΔE on the angle β , which rotates the EFG from position 1 into position 2 ($\theta_D = 215 \text{ K}$)

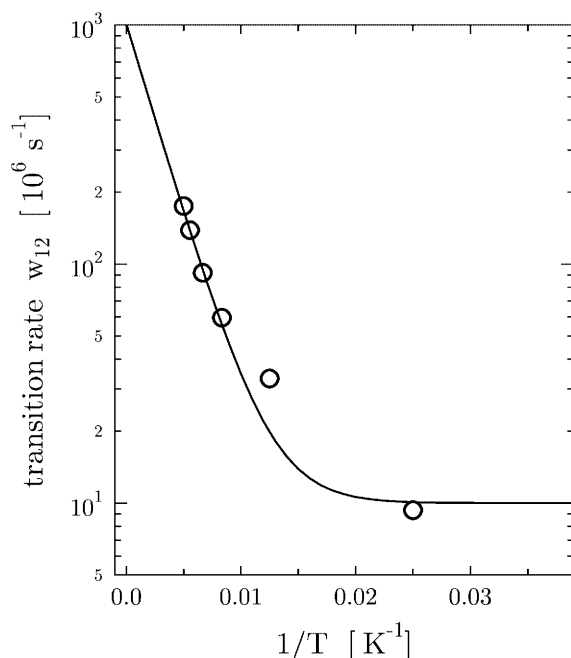


Fig. 7. Arrhenius plot of the EFG transition rates for $\theta_D = 215$ K. The solid line is a fit by the expression in Eq. 7

A comparison with the energy barrier quoted by Keller and Debrunner (1980) for the two-state conformational relaxation observable in the temperature range 200–245 K reveals that these are protein-specific motions which are obviously active in that temperature range.

Conclusion

We have successfully applied NFS using synchrotron radiation to demonstrate that the FeO_2 moiety in MbO_2 undergoes thermally activated structural disorder, i.e. the terminal O-atom in FeO_2 jumps among two possible positions which causes stochastic fluctuations of the EFG. Since the relaxation rate and the quadrupole precession frequency are of the same order of magnitude in the temperature range 3–200 K, the coherent quantum beat pattern of the NFS spectra is measurably affected by the dynamic structural disorder of the FeO_2 moiety.

In addition, we have shown that temperature dependences of the quadrupole splitting of MbO_2 and deoxyMb, though being phenomenologically very similar, are based on completely different physical mechanisms.

Acknowledgements We thank F.G. Parak (TU Munich) for providing us with the myoglobin samples. This work was supported by the German Federal Ministry of Education and Research (BMBF) under grant no. 05 SK8FLA8.

References

- Bade D, Parak F (1978) Mössbauer spectroscopy on oxygenated sperm whale myoglobin: evidence for an $\text{Fe}^{3+}\text{-O}_2^-$ coupling at the active center. *Z Naturforsch C* 33:488–494
- Baron AQR (1995) Report on the X-ray efficiency and time response of a 1 cm² reach through avalanche diode. *Nucl Instrum Methods A* 352:665–667
- Bizzarri AR, Iakovleva OA, Parak F (1995) Spin-lattice relaxation in Mössbauer spectra of metmyoglobin: investigations of crystals, water and water-glycerol solutions. *Chem Phys* 191:185–194
- Boso B, Debrunner PG, Wagner GC, Inubushi T (1984), High-field, variable temperature Mössbauer effect measurements on oxyhemoproteins. *Biochim Biophys Acta* 791:244–251
- Eicher H, Bade D, Parak F (1976) Theoretical determination of the electronic structure and the spatial arrangement of ferrous iron in deoxygenated sperm whale myoglobin and human hemoglobin from Mössbauer experiments. *J Chem Phys* 64:1446–1455
- Haas M, Realo E, Winkler H, Meyer-Klaucke W, Trautwein AX, Leupold O, Rüter HD (1997) Nuclear resonant forward scattering of synchrotron radiation by randomly oriented iron complexes which exhibit nuclear Zeeman interaction. *Phys Rev B* 56:14082–14088
- Haas M, Realo E, Winkler H, Meyer-Klaucke W, Trautwein AX (2000a) SYNFOSS. In: Gerdau E, de Waard H (eds) Nuclear resonant scattering of synchrotron radiation, part B. Baltzer, Bussum, The Netherlands, pp 189–195
- Haas M, Realo E, Winkler H, Meyer-Klaucke W, Trautwein AX, Leupold O (2000b) Paramagnetic relaxation as seen by nuclear resonant forward scattering of synchrotron radiation. *Phys Rev B* 61:4155–4159
- Herman ZS, Loew GH (1980) A theoretical investigation of the magnetic and ground-state properties of model oxyhemoglobin complexes. *J Am Chem Soc* 102:1815–1821
- Kagan Yu (1999) Theory of coherent phenomena and fundamentals of nuclear resonant scattering. In: Gerdau E, de Waard H (eds) Nuclear resonant scattering of synchrotron radiation, part A. Baltzer, Bussum, The Netherlands, pp 83–126
- Kalvius GM, Parak F (1977) Anwendung des Mößbauereffekts auf Probleme der Biophysik. In: Hoppe W, Lohmann W, Markl H, Ziegler H (eds) Springer, Berlin Heidelberg, pp 112–126
- Keller H, Debrunner PG (1980) Evidence of conformational and diffusional mean square displacements in frozen aqueous solution of oxymyoglobin. *Phys Rev Lett* 45:68–71
- Keppler C, Achterhold K, Ostermann K, van Bürck U, Chumakov AI, Rüffer R, Sturhahn W, Alp EE, Parak FG (2000) Nuclear forward scattering of synchrotron radiation by deoxymyoglobin. *Eur Biophys J* 29:146–152
- Leupold O, Winkler H (1999) Relaxation experiments with synchrotron radiation. In: Gerdau E, de Waard H (eds) Nuclear resonant scattering of synchrotron radiation, part A. Baltzer, Bussum, The Netherlands, pp 571–593
- Maeda Y, Harami T, Morita Y, Trautwein A, Gonser U (1981) Mössbauer studies on O_2 and CO binding to the heme iron in myoglobin. *J Chem Phys* 75:36–43
- Phillips SEV (1980) Structure and refinement of oxymyoglobin at 1.6 Å resolution. *J Mol Biol* 142:531–554
- Schappacher M, Richard L, Fischer J, Weiss R, Bill E, Montiel-Montoya R, Winkler H, Trautwein AX (1987) Synthesis, structure and spectroscopic properties of two models for the active site of the oxygenated state of cytochrome P450. *Eur J Biochem* 168:419–429
- Smirnov GV, Kohn VG (1995) Theory of nuclear resonant scattering of synchrotron radiation in the presence of diffusive motion of nuclei. *Phys Rev B* 52:3356–3365
- Spartalian K, Lang G (1980) Oxygen transport and storage materials. In: Cohen RL (ed) Applications of Mössbauer spectroscopy, vol II. Academic Press, New York, pp 249–279

- Spartalian K, Lang G, Collman JP, Gagne RR, Reed CA (1975) Mössbauer spectroscopy of hemoglobin model compounds: evidence for conformational excitation. *J Chem Phys* 63:5375–5382
- van Bürck U, Siddons DP, Hastings JB, Bergmann U, Hollatz R (1992) Nuclear forward scattering of synchrotron radiation. *Phys Rev B* 46:6207–6211
- Vojtěchovský J, Chu K, Berendzen J, Sweet RM, Schlichting I (1999) Crystal structures of myoglobin-ligand complexes at near-atomic resolution. *Biophys J* 77:2153–2173
- Winkler H, Schulz C, Debrunner PG (1979) Spin fluctuation rates from Mössbauer spectra of high-spin ferrous rubredoxin. *Phys Lett A* 69:360–363